Colloids and Surfaces B: Biointerfaces xxx (2016) xxx–xxx

Contents lists available at ScienceDirect

Colloids and Surfaces B: Biointerfaces

journal homepage: www.elsevier.com/locate/colsurfb

Indirect immunoassay on functionalized silicon surface: Molecular arrangement, composition and orientation examined step-by-step with multi-technique and multivariate analysis

Katarzyna Gajos[a,*], Andrzej Budkowski[a], Varvara Pagkali[b], Panagiota Petrou[b], Monika Biernat[a], Kamil Awsiuk[a], Jakub Rysz[a], Andrzej Bernasik[c], Konstantinos Misiakos[d], Ioannis Raptis[d], Sotirios Kakabakos[b]

[a] M. Smoluchowski Institute of Physics, Jagiellonian University, Łojasiewicza 11, 30-348 Kraków, Poland
[b] Institute of Nuclear & Radiological Sciences & Technology, Energy & Safety NCSR Demokritos, P. Grigoriou & Neapoleos St., Aghia Paraksevi 15310, Athens, Greece
[c] Faculty of Physics and Applied Computer Science, AGH University of Science and Technology, Mickiewicza 30, 30-059 Kraków, Poland
[d] Department of Microelectronics, Institute of Nanoscience and Nanotechnology, NCSR Demokritos, P. Grigoriou & Neapoleos St., Aghia Paraksevi 15310, Athens, Greece

ARTICLE INFO

Article history:
Received 12 July 2016
Received in revised form 11 October 2016
Accepted 3 November 2016
Available online xxx

Keywords:
Indirect immunoassay
Antibody orientation
Biosensor functionalization
TOF-SIMS
Principal Component Analysis
Surface analysis

ABSTRACT

The arrangement, composition and orientation of immunoreagents employed in an indirect immunoassay for determination of mycotoxin OchraToxin A (OTA) are specified for Si_3N_4 substrate, aiming to imitate biosensor transducers made of the same material. Si_3N_4 surfaces are examined after modification with (3-aminopropyl)triethoxysilane, spotting with OTA-ovalbumin conjugate (probe), blocking with bovine serum albumin, reaction with a mouse monoclonal antibody against OTA and, finally, reaction with a goat anti-mouse secondary antibody. Atomic force micrographs, their autocorrelation and height histogram parameters, show the stepwise development of a multi-component monolayer covered by groups of secondary antibody molecules. Time-Of-Flight Secondary Ion Mass Spectrometry reveals the composition of probe and blocking protein, as well as their partial desorption during the primary immunoreaction. Ellipsometry provides surface amount of all proteins, increasing step-by-step from 0.7 to 6.9 mg/m^2. In addition, ellipsometry combined with TOF-SIMS reveals the mass loadings of different molecules in the intermediate and the final overlayer. Based on this, some orientations of the immobilized molecules are proposed and a molar ratio of ~2.5 for secondary to primary antibody is calculated. The orientations of the primary and secondary antibody are further clarified by Principal Component Analysis of TOF-SIMS data, through which a side-on and a head-on orientation is deduced for the primary and the secondary antibody, respectively. These findings demonstrate how the combination of multiple surface analysis techniques can provide insight on the arrangement, composition and orientation of biomolecules in the course of multi-step procedures employed in biosensors.

1. Introduction

Since their discovery over 50 year ago, immunochemical methods have become one of the most powerful analytical tools [1], further exploited by the massive development of immunosensors which have found application in areas ranging from biomedical diagnostics to food safety and drug screening [2].

For silicon-based immunosensors, the surface should be appropriately functionalized prior to the immobilization of the specific immunoreagents, whereas a blocking step should be performed prior to immunoreaction to eliminate non-specific binding of reagents during the immunoreaction. The immunosensor analytical performance depends on the arrangement/orientation of immunoreagents on its surface as well as the amount of immobilized molecules. Commonly, *molecular arrangement* is concluded from spectroscopic [3–6], quartz crystal microbalance [7] or Atomic Force Microscopy data [4,6,8,9]. Nevertheless, all these approaches seem not sufficient to provide insight of what is happening onto the surface, when different molecules are involved which are

* Corresponding author.
E-mail address: katarzyna.gajos@doctoral.uj.edu.pl (K. Gajos).

http://dx.doi.org/10.1016/j.colsurfb.2016.11.009
0927-7765/

not only introduced but also partly removed from the surface during the successive modification/immunoreaction steps [10]. Therefore, surface examination with a method that could provide *discrimination between immobilized onto surface molecules*, such as Time-of-Flight Secondary Ion Mass Spectrometry, is expected to provide valuable information and help to improve immunosensors performance. In addition, such a surface examination after each functionalization and assay steps is rarely provided by the usually applied surface characterization methods [11].

Here, such a *step-by-step surface characterization* is applied in order to define *molecular arrangement* and *composition* during the course of an *indirect immunoassay* for the detection of mycotoxin, OchraToxin A (OTA). The assay is accomplished by immobilization of an OTA conjugate with ovalbumin on the surface, followed by immunoreaction with a monoclonal anti-OTA antibody (primary antibody) and a secondary antibody as a mean to increase the specific signal. It should be noted that although several investigations have been performed to define the orientation of immobilized antibodies (e.g. [5–7,9,12–14]), this is the first time the research is extended to cover *molecular orientation of* both *the primary and secondary antibody*, observed directly on functionalized surface in the course of an indirect immunoassay, and compared with the situation on reference surfaces spotted with these antibodies. Thus, in the present study, direct determination of antibody orientation is provided by Principal Component Analysis of TOF-SIMS data [4,12], performed for multi-component protein overlayers.

2. Experimental section

2.1. Materials

Silicon wafers were purchased from Si-Mat (Kaufering, Germany). 3-aminopropyltriethoxysilane (APTES), bovine serum albumin (BSA), and ovalbumin (OVA) were purchased form Sigma-Aldrich (Darmstadt, Germany). The synthesis of OTA-OVA conjugate was performed as described in a previous publication [15]. The mouse monoclonal anti-OTA antibody (anti-OTA Mab; isotype IgG1, κ) was purchased from Soft Flow Hungary Ltd. (Hungary). Affinity purified polyclonal goat anti-mouse IgG antibody (secondary antibody) was from Merck Millipore (Darmstadt, Germany). The water used throughout the study was double distilled.

2.2. Surface functionalization and assay protocol

The biofunctionalization and immunoassay steps are shown schematically in Fig. 1. Firstly, Si_3N_4 surfaces **(1)**, cleaned and hydrophilized with oxygen plasma, were immersed in a 0.5% (v/v) aqueous APTES solution for 2 min, followed by gentle washing with distilled water, drying under N_2 stream and curing for 20 min at 120 °C. Then, a 200 μg/mL OTA-OVA solution in 50 mM carbonate buffer, pH 9.2 was spotted **(2)** (over 7 mm × 7 mm areas) on the surfaces using the BioOdyssey Calligrapher Mini Arrayer (Bio-Rad Laboratories, Inc.) [10]. The spotted samples were incubated in a humidity chamber for 18 h and washed with a 10 mM Tris-HCl buffer, pH 8.25, and distilled water. Blocking **(3)** was performed by immersing the samples in a 10 mg/mL BSA solution in 0.1 M $NaHCO_3$, pH 8.5, for 2 h followed by washing and drying as previously. Reaction with the primary antibody **(4)** was performed through incubation of the samples for 1 h with a 4 μg/mL solution of anti-OTA Mab in 50 nM Tris-HCl buffer, pH 7.8, containing 9 g/L NaCl and 5 g/L BSA (assay buffer). After that, the samples were washed and dried as previously, and then incubated with a 10 μg/mL secondary antibody solution in assay buffer **(5)** for 1 h. Additionally, reference samples were prepared by spotting directly solutions of 4 μg/mL of anti-OTA Mab **(r4)** or 10 μg/mL of secondary antibody in 50 mM carbonate buffer, pH 9.2 **(r5)**. The reference samples were washed with buffer and distilled water and dried under N_2 stream.

2.3. AFM surface examinations

Agilent 5500 microscope working in a non-contact mode (resonant frequency ~70 kHz, tip radius ~7 nm, spring constant ~2 N/m) under ambient conditions was used to acquire AFM images from different areas of each sample. The WSxM software was used (downloadable at http://www.nanotec.es) for processing of the images.

2.4. TOF-SIMS surface characterization

A TOF.SIMS 5 (ION-TOF GmbH) instrument equipped with Bi_3^+ ion clusters (30 keV liquid metal ion gun) was used. Ion dose density was lower than 10^{12} ion/cm^2 (static mode). A low energy electron flood gun was used for charge compensation. High mass resolution positive ion static TOF-SIMS spectra were acquired from six non-overlapping 100 μm × 100 μm areas of each sample. Mass calibration was performed with H^+, H_2^+, CH^+, $C_2H_2^+$ and $C_4H_5^+$ peaks. A minimal mass resolution ($m/\Delta m$) > 5300 at $C_4H_5^+$ was obtained. To investigate differences in molecular coverage rather than changes in relative composition, TOF-SIMS data that have been obtained with dose density and primary beam current identical for all measurements are used without normalization. Surface sensitivity of TOF-SIMS experiments using Bi_3^+ primary ions was described [16] by exponential decay of signal intensity as a function of organic overlayer thickness, and characterized by escape depth of secondary ions of ~4 nm [16]. This value corresponds to uniform protein layer [11] with surface density of ~5.5 mg/m^2.

2.5. Multivariate TOF-SIMS analysis with PCA

Principal Component Analysis was performed for the positive TOF-SIMS spectra using the PLS Toolbox (Eigenvector Research, Manson, WA) for MATLAB (MathWorks, Inc., Natick, MA). The intensities of selected peaks from each spectrum were normalized to the sum of selected peaks and mean-centred prior to running PCA.

2.6. Ellipsometry measurements

The Sentech SE800 (Sentech Instruments GmBH) Spectroscopic Ellipsometer (wavelength range of 320–700 nm, fixed angle of incidence ~70°) along with the SpectraRay 3 software was used. Average thickness was estimated by fitting model predictions to Ψ and Δ relations, assuming the Cauchy dispersion formula. The three-layer model consisted of silicon substrate/Si_3N_4/mixed SiO_2 and APTES layer/protein overlayer. Fixed refractive index values n = 3.87 for Si, 2.01 for Si_3N_4 [17], 1.46 for both SiO_2 and APTES [18], and 1.53 for proteins [19] were used. The thickness of Si_3N_4 layer (122.5 nm), as well that of mixed SiO_2 and APTES layer (6.3 nm), both obtained from measurements performed on a bare silanized surface, were taken into account to fit the thickness of protein layer.

3. Results and discussion

3.1. Multi-step procedure for silicon surface modification leading to indirect assay

The reagents and assay procedure employed in the present study have been previously applied for the determination of OTA in beer samples employing an array of integrated on silicon Mach-Zehnder Interferometric sensors based on Si_3N_4 waveguides [10,15]. Thus,

Please cite this article in press as: K. Gajos, et al., Indirect immunoassay on functionalized silicon surface: Molecular arrangement, composition and orientation examined step-by-step with multi-technique and multivariate analysis, Colloids Surf. B: Biointerfaces (2016), http://dx.doi.org/10.1016/j.colsurfb.2016.11.009

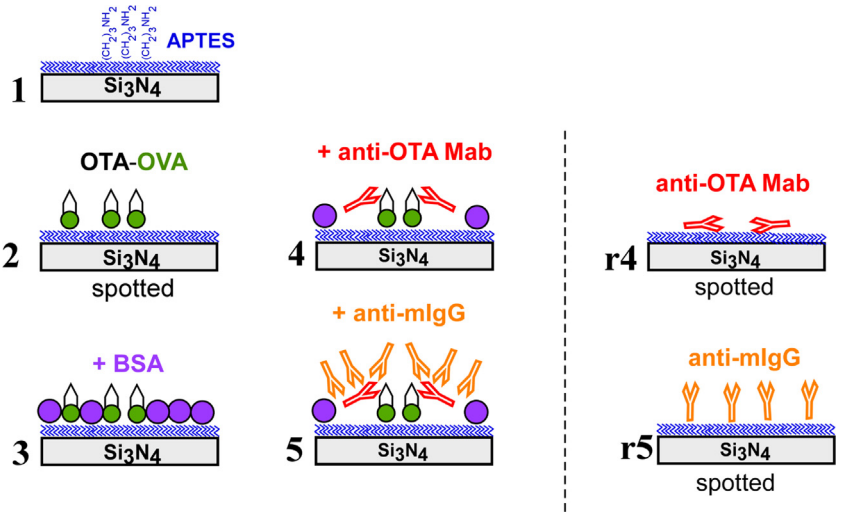

Fig. 1. Schematic of the procedure employed for biofunctionalization of Si_3N_4 surfaces (**1**–**3**) and indirect immunoassay for detection of mycotoxin OTA (**4**-**5**). Si_3N_4 surfaces were modified with APTES (**1**), spotted with OTA-OVA conjugate (**2**), blocked with BSA (**3**), and reacted first with the anti-OTA Mab (**4**), and then with a secondary antibody (anti-mIgG) (**5**). Reference samples were directly spotted with primary (**r4**) and secondary antibody (**r5**).

in the present work Si_3N_4 surfaces prepared in a similar way to integrated waveguides were employed in order to mimic the molecular arrangements in the particular sensor. In the aforementioned sensor, a competitive immunoassay format, schematically depicted in Fig. 1, is applied to determine traces of mycotoxin OTA in beer samples through incubation of calibrators or samples with the anti-OTA Mab prior to reaction with the immobilized onto the sensors surface OTA-OVA probe. Thus, all the surfaces examined in the present study correspond to zero calibrator.

The procedure of Si_3N_4 surface modification (Fig. 1) consists of: **(1)** chemical activation with amino-silane (APTES); **(2)** immobilization of the probe OTA-OVA (spotted from solution); **(3)** blocking of non-specific binding with bovine serum albumin (BSA); **(4)** specific binding of primary mouse monoclonal antibody against OTA (anti-OTA Mab); **(5)** binding of secondary goat anti-mouse IgG antibody (anti-mIgG). Amino-silanized Si_3N_4 surfaces spotted with primary **(r4)** and secondary antibody **(r5)** are used as references. The specificity of anti-OTA Mab binding to the silicon surfaces after functionalization with OTA-OVA conjugate [steps **(1)**–**(3)**] was confirmed by the negligible response of Mach-Zehnder Interferometric sensors spotted [in step **(2)**] with OVA instead of the OTA-OVA conjugate, as well as by the fact that the response of OTA-OVA spotted sensors increased as the concentration of OTA-OVA conjugate in the spotting solution was increased, as shown in our relevant publication [15]. Moreover, it should be noted that the sensor blocking procedure (and hence of plain Si_3N_4 surfaces) and composition of assay buffer has been optimized in order to eliminate non-specific binding of both the anti-OVA Mab and secondary antibody.

3.2. Molecular arrangement and composition after functionalization and assay steps

3.2.1. Overlayer nanostructure visualized with AFM

AFM topographic images recorded after each one of the successive functionalization and immunoassay steps (Fig. 2a) reveal laterally uniform nanostructured molecular overlayers. Lateral nanostructure is described by the mean size of surface features *2whm* (Fig. 2b) provided by a radial averaged autocorrelation function computed for each AFM micrograph [11]. In turn, vertical nanostructure in an AFM image is characterized by the parameters of height distribution [11], such as average height $\langle h \rangle$ (Fig. 2c) and the root-mean-square surface roughness *RMS* (Fig. 2d).

Chemical activation of Si_3N_4 surface with APTES (**1**) yields self-assembled amino-silane monolayers (see Fig. 2) characterized by nanostructure parameters values of $\langle h \rangle = 0.85$ (± 0.10) nm and $RMS = 0.21$ (± 0.01) nm, identical to those reported in previous publications [11]. Subsequent spotting with the OTA-OVA probe (**2**) leads to partial surface coverage with proteins with distinct increments of $\Delta\langle h \rangle \sim 1.0$ nm and $\Delta RMS \sim 0.4$ nm. Well marked surface features with mean size *2whm* ~19 nm, correspond to OVA molecules which have a predicted apparent size of 19 and 23 nm for half-spherical and spherical shapes of immobilized molecules, respectively, as calculated taking into account the molecule nominal dimensions $9.4 \times 3.6 \times 3.6\ nm^3$ [20] and the broadening caused by the AFM tip (with 7 nm radius) [11]. The subsequent treatment of the surface with BSA **(3)** increases the surface coverage with proteins, resulting in increments of $\Delta\langle h \rangle \sim 2.2$ nm and $\Delta RMS \sim 0.3$ nm. Nevertheless, the mean size of surface features is hardly altered ($\Delta 2whm \sim 1$ nm), since the nominal dimensions ($9.0 \times 5.5 \times 5.5\ nm^3$ [21]) and apparent size of BSA (18–22 nm provided by the relevant models [11]) are similar to those of OVA.

The first immunoassay step **(4)**, that involves exposure of the functionalized surface to primary antibody, induces hardly any change in both average height $\Delta\langle h \rangle \sim 0.2$ nm and mean size of surface features $\Delta 2whm \sim 1$ nm, accompanied by minor increment in surface roughness $\Delta RMS \sim 0.2$ nm (Fig. 2). These parameters, as well as the original AFM images that are similar to those of step **(3)**, suggest that the primary antibody is incorporated into a *multi-component monolayer*. In addition, the primary immunoreaction is accompanied by partial desorption of blocking protein (BSA) and probe (OTA-OVA) (discussed in the Section 3.2.2). This accords with the minimal change in *2whm* observed, especially if one considers the fact that apparent size of IgG molecule, 25–28 nm (predicted according to [11] for a nominal size of $14.5 \times 8.5 \times 4.5\ nm^3$ [22]) is not much larger compared to that of the two albumins (e.g. up to 23 nm for OVA).

Finally, the second immunoreaction **(5)** results in a significant increase of vertical nanostructure parameters, $\Delta\langle h \rangle \sim 1.8$ nm and $\Delta RMS \sim 0.5$ nm, accompanied by a huge expansion of lateral nanostructure, reflected by nearly two-fold increase in the mean size of surface features *2whm* ~40 nm (see Fig. 2b). The *2whm* value is the same with the apparent size predicted for a group of two IgG molecules [11]. These striking changes in biomolecular overlayer reflect *efficient affinity binding* between primary and secondary antibodies, resulting in coverage of the multi-component protein

Please cite this article in press as: K. Gajos, et al., Indirect immunoassay on functionalized silicon surface: Molecular arrangement, composition and orientation examined step-by-step with multi-technique and multivariate analysis, Colloids Surf. B: Biointerfaces (2016), http://dx.doi.org/10.1016/j.colsurfb.2016.11.009

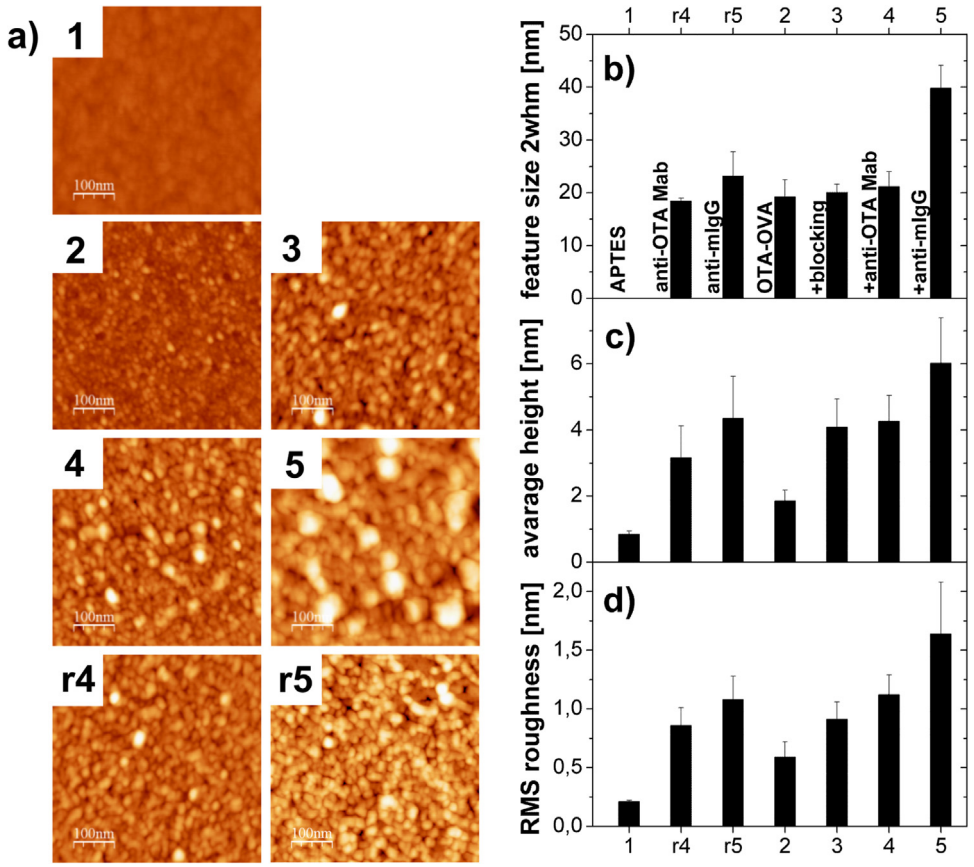

Fig. 2. (a) Representative topographic AFM micrographs (with identical height-range of 10 nm) and (b–d) nanostructure parameters obtained from the Si_3N_4 surfaces **(1-5)** after each one of the successive functionalization/immunoassay steps. The respective data for reference samples (**r4**, **r5**) are also provided. The nanostructure parameters calculated were: (b) the mean size of surface features, *2whm*, (c) the mean value of average height <*h*>, and (d) the root mean square roughness *RMS*. Error bars are standard deviations determined from 4 to 6 AFM images or height histograms of the same surface.

monolayer formed after the primary immunoreaction by grouped anti-mIgG molecules. The coverage of this additional protein layer must be relatively high, since it is not well penetrated by the AFM tip resulting in a somewhat limited height increment, Δ<*h*>, when compared to IgG dimensions.

Furthermore, the nanostructures formed on the reference surfaces directly spotted with anti-OTA Mab (**r4**) or anti-mIgG (**r5**) are comparable (see Fig. 2) to those determined for protein monolayers formed on the surface prior to (**3**) and after the first immunoreaction (**4**). However, the average height of anti-OTA Mab overlayer (**r4**) is smaller by about one-quarter of that of anti-mIgG (**r5**), reflecting lower surface coverage, possibly due to the lower concentration of the first in the spotting solution. Moreover, the mean size of surface features *2whm* for sample (**r4**) is distinctively smaller (∼18 nm), than that determined for sample (**r5**) (∼23 nm). The former result accords with the size determined by AFM for Fc ($7.0 \times 6.3 \times 3.1$ nm^3 [23]) or Fab ($8.2 \times 5.0 \times 3.8$ nm^3 [23]) antibody fragments, while the latter with the apparent size of whole IgG molecule (25–28 nm). Recent AFM experiments show that the different IgG fragments can be resolved as separate surface features in layers of IgG molecules with specific orientations [8]. Thus, these different *2whm* values (Fig. 2b) could point to *different molecular orientation* of anti-OTA Mab (**r4**) and anti-mIgG molecules (**r5**), a suggestion confirmed by the results presented in Sections 3.2.3 and 3.3.

3.2.2. Overlayer composition of probe and blocking protein examined with TOF-SIMS

TOF-SIMS can distinguish between ion fragments of different amino acids. When the concentration and arrangement of amino acids in different protein molecules are not the same, characteristic TOF-SIMS signals can be ascribed to different proteins. The composition of OVA, BSA and model antibody provided in Table 1 [4,24] indicates amino acids with distinguishably high concentration in some of these proteins, such as methionine (4.4% in OVA, 0.7% in BSA, 2.0% in antibody) and glutamic acid (8.8% in OVA, 10.1% in BSA, 5.1% in antibody). Thus, the respective ion fragments are suggested as characteristic TOF-SIMS signals for OVA (Fig. 3a) and OVA and BSA (Fig. 3b), respectively. Comparison of the experimental results (Fig. 3) obtained for the surfaces functionalized with OTA-OVA (**2**) and BSA (**3**) and the reference surfaces (**1** or APTES, **r4**, **r5**) show that indeed the methionine TOF-SIMS signal is specific for OVA; while the glutamic acid signal is characteristic for both albumins (OVA and BSA), with small contributions from antibodies (anti-OTA Mab, anti-mIgG). Similar analysis has failed to provide a mass signal specific for the two antibodies.

The TOF-SIMS signals presented in Fig. 3 enable an insight into composition of OVA and cumulative albumin (OVA and BSA) in the protein overlayer after the different biofunctionalization and assay steps. Thus, the blocking procedure (**3**) introduces BSA molecules at the surface while preserving the existing coverage with OTA-OVA probe. Subsequently, both *probe* (OTA-OVA) *and blocking protein* (BSA) are partly *desorbed* during the primary immunoreaction step creating a multi-component monolayer (**4**). Then, the secondary antibody molecules cover the multi-component monolayer without affecting the pre-existing composition (**5**). Taking it overall, the picture provided by TOF-SIMS (Fig. 3) is consistent with that formed by the AFM analysis of the respective surfaces (Fig. 2). A more precise analysis of the surface composition and structure is attempted

Please cite this article in press as: K. Gajos, et al., Indirect immunoassay on functionalized silicon surface: Molecular arrangement, composition and orientation examined step-by-step with multi-technique and multivariate analysis, Colloids Surf. B: Biointerfaces (2016), http://dx.doi.org/10.1016/j.colsurfb.2016.11.009

Table 1
Comparison of amino acid composition (%) of OVA [24], BSA [24] and model antibody [4] (see Supplementary data for similar analysis made for the composition of model antibody reported in other publications [31,32]). The last column marks the amino acids with a composition ratio in Fc to $F(ab')_2$ fragments larger than 1.5 (based on Ref. [4]).

amino acids	OVA (%)	BSA (%)	Antibody (%)	Fc>>Fab ($Fc/F(ab')_2 > 1.5$)
alanine/ala	9.1	8.0	5.1	
arginine/arg	3.9	4.0	2.8	
(Asparagine)/(Asn)	3.9	2.4	4.6	
aspartic acid/asp	4.4	6.9	4.8	
cysteine/cys	0.3	6.0	2.0	
(Glutamine)/(Gln)	3.9	3.4	4.3	
glutamic acid/glu	8.8	10.1	5.1	
(Glycine)/(Gly)	4.9	2.7	5.4	
histidine/his	1.8	2.9	1.9	+
isoleucine/ile	6.5	2.4	3.4	+
leucine/leu	8.3	10.5	5.9	
lysine/lys	5.2	10.1	6.2	+
methionine/met	4.4	0.7	2.0	
phenylalanine/phe	5.2	4.6	3.9	+
PROLINE/PRO	3.6	4.8	6.3	+
SERINE/SER	9.8	4.8	12.5	
THREONINE/THR	3.9	5.7	8.8	
TRYPTOPHAN/TRP	0.8	0.3	2.0	
TYROSINE/TYR	2.6	3.4	4.6	
(Valine)/(Val)	8.0	6.2	8.3	

Notation: all-caps for both antibody/BSA and antibody/OVA > 1.25; lowercase for either BSA/antibody or OVA/antibody > 1.25; underlined for $Fc/(Fab')_2 > 1.5$; names and abbreviations in brackets for other amino acids.

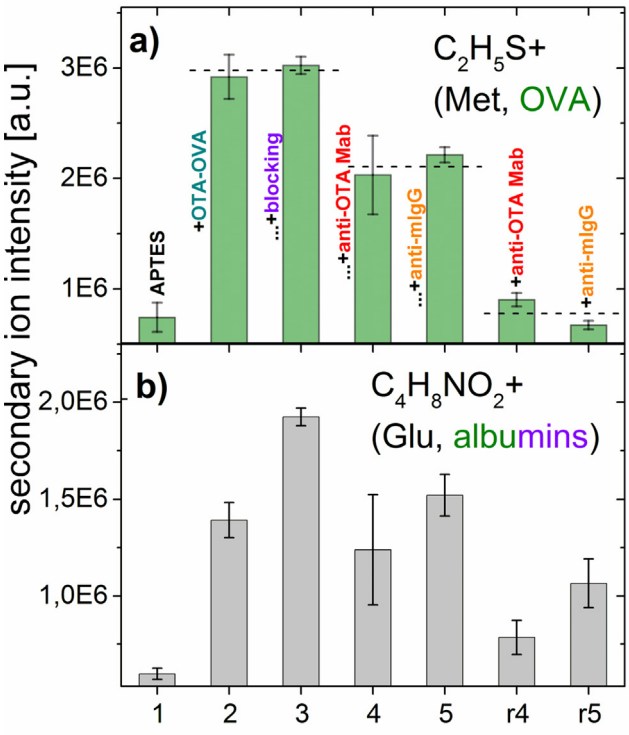

Fig. 3. TOF-SIMS analysis of multi-molecular layers formed on Si_3N_4 surfaces after each one of biofunctionalization/immunoassay steps (**1**–**5**) as well as for the reference samples (**r4**, **r5**). The signal intensities of secondary ions: (a) $C_2H_5S^+$ (from methionine) – specific for OVA, and (b) $C_4H_8NO_2^+$ (from glutamic acid) – characteristic for both albumins (OVA, BSA; with small contributions from antibodies) are provided. Error bars are standard deviations determined from 6 spectra acquired for each sample.

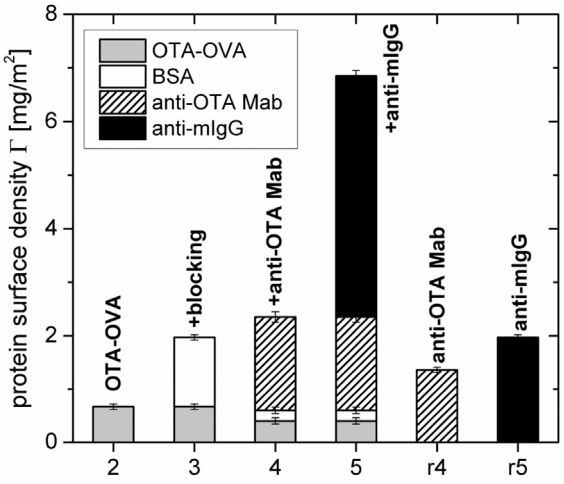

Fig. 4. Total protein surface density Γ (heights of stacked columns) and component mass loadings of different biomolecules (gray, white, hatched and black columns for OTA-OVA, BSA, primary and secondary antibody, respectively) determined with ellipsometry and evaluated with TOF-SIMS (Fig. 3) after each one of the individual biofunctionalization/immunoassay steps taking place on the Si_3N_4 surfaces. Error bars are standard deviations determined from 3 ellipsometric measurements of the same surface.

in the Section 3.2.3, where the TOF-SIMS data are combined with ellipsometry results.

3.2.3. Determination of proteins amount on the silanized surfaces by ellipsometry

The thickness D of protein overlayer was determined by ellipsometry using the multi-layer model described in Section 2.6. Then, the protein surface density Γ was estimated after each one of the surface modification steps (Fig. 4) following the Cuypers one-component approach [25]:

$$\Gamma = D * \rho = d * (M/A) * (n_p^2 - 1)/(n_p^2 + 2) \quad (1)$$

A value of refractive index, $n_p = 1.53$ [19], and a ratio of molecular weight to molar refractivity M/A = 4.14 g/mL [25] are assumed for all the proteins [19,25].

3.2.3.1. Mass loadings of different biomolecules. Based on AFM and TOF-SIMS results, it has been concluded that the addition of new molecules upon blocking (**3**) and secondary immunoreaction (**5**) is not accompanied by any distinct change of the pre-existing surface protein coverage. On the other hand, the surface coverage by the two albumins, OTA-OVA and BSA, is reduced during the primary immunoreaction (**4**). To evaluate the mass loadings of different pro-

teins on the formed multi-component layer, the ellipsometric data are considered in combination with the TOF-SIMS signal intensities (Fig. 3), $I'(\mathbf{n}) = I(\mathbf{n}) - I(\mathbf{1})$, determined always with reference to bare silanized surface (**1**). Also, the assumption is made that the ratio of component contribution to TOF-SIMS signal and component mass loading, $I'^{component}(\mathbf{n})/\Gamma'^{component}(\mathbf{n})$, for sample (**4**) is the same with those of samples with pure components, i.e., sample (**2**) for the signal $C_2H_5S^+$ from OTA-OVA, and samples (**3**) and (**r4**) for the signal $C_4H_8NO_2^+$ corresponding to the two albumins and primary antibody, respectively. This is equivalent to assuming that TOF-SIMS spectra show linear correlation with organic surface composition [26,27].

The ellipsometric data provide by subtraction for the steps (**2**) and (**3**) a surface density of 0.7 and 1.3 mg/m^2 for OTA-OVA and BSA, respectively (see gray and white columns in Fig. 4). Both these mass loadings, when calculated as described above, are reduced upon the first immunoreaction (**4**) to 0.4 for OTA-OVA and 0.2 mg/m^2 for BSA. This leads to a value of 1.8 mg/m^2 for the primary antibody (hatched column in Fig. 4) in order to match a total protein amount Γ of 2.4 mg/m^2. Taking into account that these molecular mass loadings are preserved upon the second immunoreaction (**5**) and that the total amount of protein determined equals 6.9 mg/m^2, a surface density of 4.5 mg/m^2 is calculated for the secondary antibody. In turn, mass loading of 1.4 mg/m^2 and 2.0 mg/m^2, are determined for the primary and the secondary antibody, respectively, from the analysis of amino-silanized reference surfaces where the two molecules have been directly spotted.

3.2.3.2. Evaluation of immunoactivity. The determined surface amounts of secondary (anti-mIgG) and primary (anti-OTA Mab) antibody yield a binding molar ratio of ~2.5. This confirms the AFM observations, that grouped secondary antibodies (with apparent group size equal to that of two IgG molecules) cover the multi-component monolayer containing the primary antibodies. We also note, that the binding molar ratio determined in this study is similar to the value of ~2.4, calculated in a previous study for secondary anti-rabbit IgG antibody binding on rabbit gamma-globulins adsorbed to silicon surfaces [11a].

3.2.3.3. Preselection of molecular orientation of immobilized proteins. Asymmetric proteins could adapt specific orientations upon their immobilization onto solid surfaces. These orientations define which protein part is exposed to the surrounding medium, thus regulating the biological activity of the immobilized molecules [28]. The surface density Γ data can shed some light on dominant molecular orientation, as the latter specifies cross-sectional area and mass loading Γ_{ind} of individual biomolecules [6,7,9,11,21,23]. In particular, the molecular architecture of albumins indicates two orientations [20,21]: side-on (Γ_{ind} = 2.3 and 2.2 mg/m^2 for OVA and BSA, respectively) and end-on (5.7 mg/m^2 for OVA and 3.65 mg/m^2 for BSA). In turn, four distinct orientations are predicted for the antibody molecule taking into account the three lobe-shaped fragments (the two Fab and the one Fc fragment) [23]: flat-on (all three lobes attached to surface; 2.0 mg/m^2), side-on (Fc and one Fab at substrate; ~2.9 mg/m^2), end-on (Fab-up, Fc at surface; 2.6–5.5 mg/m^2) and head-on (Fc-up, both Fabs attached to the substrate; 2.6–5.5 mg/m^2).

To maximize fractional surface coverage, immobilized proteins prefer to adopt the molecular orientation that leads to a Γ_{ind} value near to surface density value Γ [28,29]. However, molecular mass loading Γ_{ind} must be reasonably larger than Γ, since close packing of adsorbed molecules cannot be achieved [28,29]. Accordingly, side-on alignment is advocated for the directly adsorbed OTA-OVA molecules (**2**) with surface density value, Γ = 0.7 mg/m^2 (cf. Γ_{ind} values), whereas for the subsequently added BSA, that leads to a cumulative mass loading of 2.0 mg/m^2 (**3**), an end-on rather than side-on dominant orientation is expected. Since the surface coverage by both albumins is reduced considerably during the immunoreaction with the primary antibody (**4**), all orientations of anti-OTA Mab (Γ = 1.8 mg/m^2) seem plausible except for flat-on orientation. Also, end-on alignment is excluded for geometrical reasons, since primary antibodies are incorporated into the multi-molecular monolayer. Thus it seems that most of the anti-OTA Mab molecules have a side-on or head-on orientation indicating binding of one or both binding sites located on the Fab fragments to the immobilized onto the surface OTA moieties. Finally, the protein monolayer created during the first immunoreaction is enveloped during the second one (**5**) by a huge amount of attached secondary antibody, 4.5 mg/m^2, that can be accommodated in a new monolayer only if the end-on or head-on orientations are adopted [7]. In turn, for the reference surfaces, a flat-on orientation is defined for the spotted primary antibody with a surface density of 1.4 mg/m^2 (**r4**), but more vertical, side-on or end-on (or head-on), orientations are indicated [7,9] for the spotted secondary antibody (**r5**) with higher mass loading of 2.0 mg/m^2. This difference could be due to the fact that the concentration of secondary antibody in the spotting solution was 2.5-times higher than the concentration of the primary antibody.

3.3. Orientation of the primary and secondary antibody and molecular arrangement from multivariate TOF-SIMS analysis

To determine subtle differences in amino acids composition between the *outermost regions* of the functionalized Si_3N_4 surfaces after the immunoreaction with primary (**4**) and secondary antibody (**5**), as compared to the situation on the reference surfaces spotted directly with these antibodies (**r4** and **r5**), multiple TOF-SIMS signals are examined simultaneously with multivariate PCA analysis (Fig. 5). The examined TOF-SIMS data set, consisting of the relative intensities of 38 amino acids fragments (listed in Fig. 6) from 24 spectra, can be visualized as 24 points in a 38-dimensional space. PCA reduces dimensionality of the data set while retaining its essential information by transforming the original signals into two principal components (PCs) that account for *uncorrelated* major variations within the data set. Thus, the PCA scores plot provided in Fig. 5a describes the surface compositions (24 points with different symbols for various surfaces) in terms of the principal components PC1 and PC2.

The first PC (PC1), that captures 86.28% of the total variance, is defined by the loadings plot presented in Fig. 6a. PC1 is loaded positively by the fragments of amino acids (marked with all-caps) that have higher abundance in the antibody than the albumin molecules (BSA and OVA, see Table 1). On the other hand, the amino acids (distinguished by lowercase) with higher abundance in the albumin (BSA or OVA) than the antibody molecule (see Table 1) contribute to the mass signals that loads PC1 negatively. While PC1 resolves antibody from albumin, the second PC (PC2) captures the largest residual variance in the data set, uncorrelated to that described by the PC1. Indeed, the loadings plot (Fig. 6b) shows that PC2 can be related to antibody orientation, as it is loaded negatively only by the dominant ion fragments of the amino acids (marked by underlined fonts) that are more abundant in the Fc than the F(ab')$_2$ fragments (see Table 1), indicating an antibody orientation that exposes the Fc fragment. In turn, the amino acids with higher abundance on the F(ab')$_2$ fragment point to other antibody orientations. It should be noted, that similar conclusions are drawn from PC1 and PC2 when amino-acid compositions for the IgG molecule from different literature sources are used [4,31,32] (see Supplementary data).

The interpretation of PC1 and PC2, based on the loadings plots (Fig. 6), could reveal subtle differences in amino acids composition between the *outermost regions* of different surfaces (Fig. 5). The determined compositions are grouped in four clusters of data

Please cite this article in press as: K. Gajos, et al., Indirect immunoassay on functionalized silicon surface: Molecular arrangement, composition and orientation examined step-by-step with multi-technique and multivariate analysis, Colloids Surf. B: Biointerfaces (2016), http://dx.doi.org/10.1016/j.colsurfb.2016.11.009

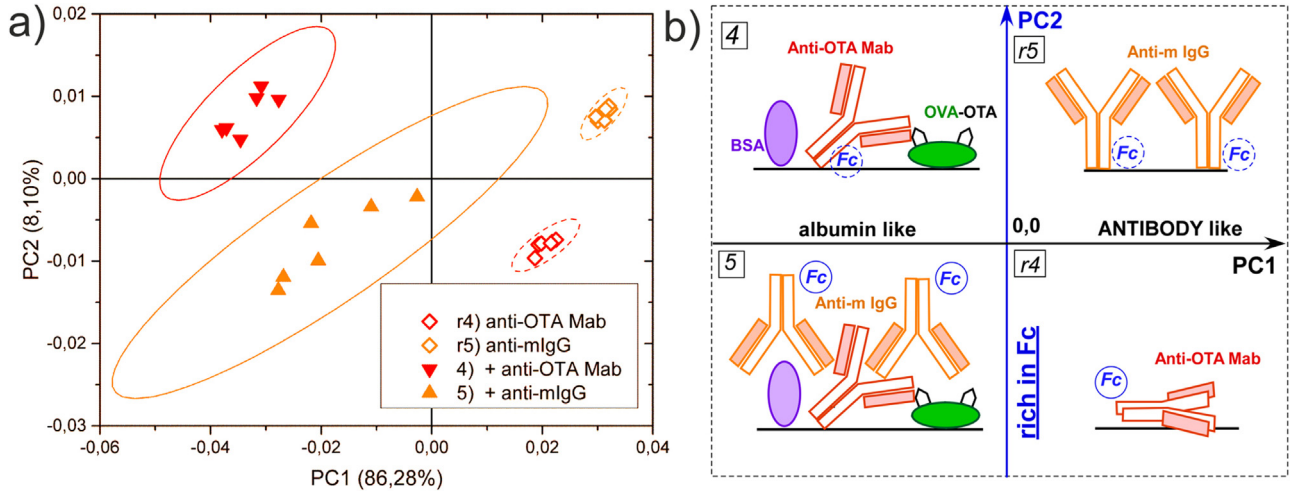

Fig. 5. (a) PCA scores plot (loadings for PC1 and PC2 are shown in Fig. 6) of the TOF-SIMS spectra recorded for functionalized Si_3N_4 surfaces after immunoreaction with primary (**4**) and secondary antibody (**5**) as well as for the reference surfaces (**r4**, **r5**) spotted directly with each one of the antibodies. The ellipses drawn around each of the grouped data points (solid lines for the surfaces (**4**), (**5**), and dashed lines for the references (**r4**), (**r5**)) represent the 95% confidence limit. (b) Molecular arrangement and orientation of primary and secondary antibody deduced for the surfaces examined with PCA in (a).

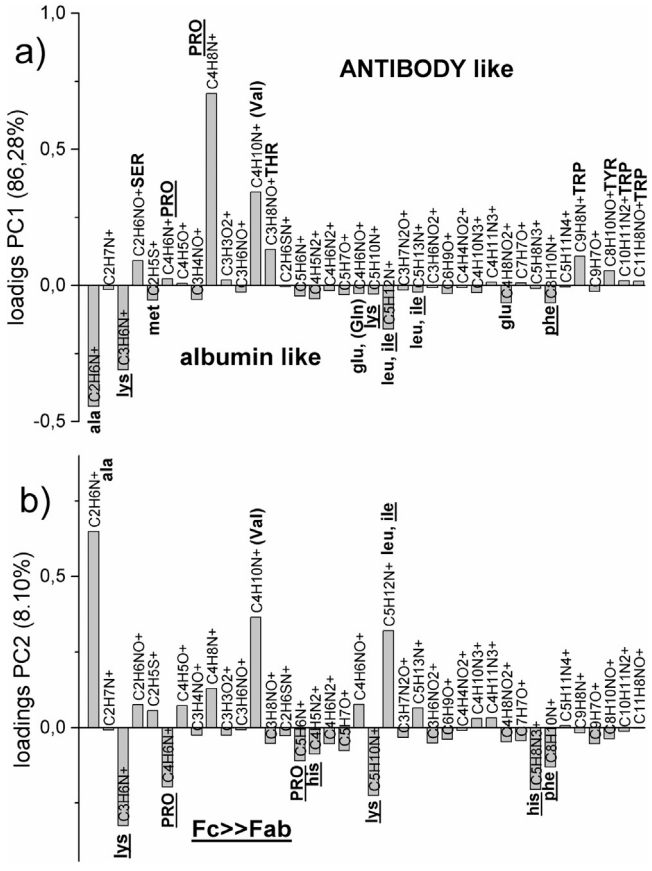

Fig. 6. Loadings plots for (a) the first and (b) the second Principal Component in Fig. 5a. Amino acids are attributed to the secondary ions based on Ref. [30] and supplemented by Ref. [4]. (a) PC1 is loaded positively by the signals from amino acids (marked with all-caps) with higher content in antibody than in albumin molecules (see Table 1). The amino acids yielding ion fragments loading negatively the PC1 (distinguished by lowercase) originate from albumin (OVA or BSA) rather than antibody molecules (Table 1). Other amino acids are marked by abbreviations given in brackets. (b) PC2 reflects the second major variation in TOF-SIMS data that is uncorrelated with that of PC1. PC2 is loaded negatively by ion fragments of the amino acids (underlined, see Table 1) characteristic for Fc fragment – indicating an antibody orientation that exposes the Fc fragment.

points, centered in different quadrants of the coordinate system PC1 vs. PC2. The first PC, resolving albumins from antibody molecules, have generally negative values for functionalized surfaces on which albumins have been immobilized (**4** and **5**), and positive values for reference surfaces spotted directly with antibodies (**r4** and **r5**). Additional coverage with secondary antibody (**5**) that reduces accessibility of albumins by TOF-SIMS, yields in negative PC1 values of lower magnitude for the cluster center.

The second PC resolves the different antibody orientations, with the exposure of Fc fragments indicated by the negative PC2 values. The sign of PC2 coordinate (see Fig. 5) changes for the data points corresponding to both the reference (**r4**, **r5**) and the indirect immunoassay surfaces (**4**, **5**). On the surfaces where the antibodies have been immobilized by direct spotting, the orientation of IgG molecules switches from *flat-on* alignment at low coverages (**r4**) to more *end-on* orientation for higher antibody surface density (**r5**). This is accompanied by reduced exposure of Fc fragments and increased exposure of Fab fragments, which leads to change of PC2 values from negative to positive. A less pronounced PC2 values change would be expected when the orientation switches to head-on or side-on alignment (alternatives suggested by ellipsometry) which correspond to more or less exposed Fc fragments, respectively.

In turn, the negative PC2 values for the cluster center corresponding to the functionalized surfaces after the second immunoreaction (see (**5**) in Fig. 5) reflect dominant *head-on*, hence Fc up, orientation of IgG molecules for the secondary antibodies that are bound to the multi-molecular monolayer containing the primary antibodies. In contrast, the positive PC2 values describe the primary antibodies that were embedded to the monolayer during the first immunoreaction (**4**), with a *side-on* orientation of the antibody molecules that leads to reduced exposure of Fc fragments. The embedment of primary antibody molecule between the BSA and OTA-OVA molecules, and the slight tilt of antibody due to specific binding of its Fab unit to exposed OTA moieties of the immobilized OTA-OVA conjugate, result to an additional shielding of the Fc fragments (see Fig. 5b). In contrast to these observations, an alternative head-on orientation, preselected also by ellipsometry for (**4**), with Fab units oriented towards the OTA-OVA conjugate, would result in negative PC2 values.

Taking it overall, our analysis shows that PCA of TOF-SIMS data specifies which molecular orientations, preselected by ellipsome-

Please cite this article in press as: K. Gajos, et al., Indirect immunoassay on functionalized silicon surface: Molecular arrangement, composition and orientation examined step-by-step with multi-technique and multivariate analysis, Colloids Surf. B: Biointerfaces (2016), http://dx.doi.org/10.1016/j.colsurfb.2016.11.009

try, are in fact acquired by the antibody molecules. In addition, the PCA shows that the dominant antibody orientation could be defined by the molar binding ratio for immunoadsorbed onto the surface antibodies (**4**, **5**) or the surface density in case of directly adsorbed onto the surface antibodies (**r4**, **r5**).

4. Conclusions

A procedure for silicon nitride surface functionalization and performance of an indirect immunoassay for detection of the mycotoxin OchraToxin A is examined *step-by-step* with multiple surface techniques including AFM, TOF-SIMS and ellipsometry. The analysis of the data received from the three techniques provides information not only about the molecular arrangement and composition of the protein layer and the changes after each step but also about the orientation of primary and secondary antibody.

Partial desorption of probe (OTA-OVA conjugate) and blocking protein (BSA) molecules is witnessed by TOF-SIMS during the immunoreaction with the primary (anti-OTA Mab) antibody. Moreover, AFM, TOF-SIMS and ellipsometry data reveal a *complex multi-component monolayer*, which accommodates primary antibodies along with the OTA-OVA and BSA molecules, and is covered by secondary antibodies after the completion of the immunoassay procedure. In addition, the AFM-based analysis resolves *specific surface features*, such as grouped secondary antibodies, that correspond to a binding molar ratio of ~2.5.

Analysis by ellipsometry and AFM, further supported by PCA analysis of TOF-SIMS data, provides also some hints about the *orientation of the immunoadsorbed primary and secondary antibody molecules* as compared to the orientations the same antibodies acquire when are directly immobilized onto the surfaces by spotting. In particular, this comparison revealed that the dominant antibody orientation is defined in the case of the immunoadsorbed antibodies by the molar binding ratio (changing from side-on to head-on as the molar binding ratio increases) or by the surface density (changing from flat-on to end-on as the surface density increases).

The concluded dominant IgG orientations result from a compromise between electrostatic and van der Waals forces [4,6,7,33,34] to which specific immunochemical reactions are ascribed. Thus, the flat-on orientation, expected for van der Waals interactions with the positively charged amino-terminated surface [4,7,33], changes into an end-on alignment as the surface coverage with the IgG increases due to accumulation of electric dipoles [4,6,33]. In turn, the combination of electrostatic interactions between the surface and the antibody Fc unit along with the specific Fab binding to the immobilized OTA-OVA molecule leads to the side-on orientation for the primary antibody and its embedment in the multi-molecular monolayer consisting also of OTA-OVA and BSA molecules. Finally, a head-on orientation is expected for the secondary antibodies that are immunoadsorbed onto the primary antibodies of the protein monolayer.

Acknowledgments

This work was supported by the EU funded project "FOODSNIFFER" (FP7-ICT8-318319) and sponsored from the Polish state funds for science in the years 2014–15 granted for the realization of co-financed international project. The equipment used was purchased thanks to the financial support of the European Regional Development Fund (POIG.02.01.00-12-023/08). One of us (K.G.) is grateful for financial support from the M. Smoluchowski Kraków Research Consortium (in the framework of the KNOW scholarship).

Appendix A. Supplementary data

Supplementary data associated with this article can be found, in the online version, at http://dx.doi.org/10.1016/j.colsurfb.2016.11.009.

References

[1] R.S. Yalow, S.A. Berson, Nature 184 (1959) 1648–1649.
[2] T. Holford, F. Davis, S. Higson, Biosens. Bioelectron. 34 (2012) 12–24.
[3] K. Awsiuk, A. Budkowski, M.M. Marzec, P. Petrou, J. Rysz, A. Bernasik, Langmuir 30 (2014) 13925–13933.
[4] H. Wang, D.G. Castner, B.D. Ratner, S. Jiang, Langmuir 20 (2004) 1877–1887.
[5] X. Zhao, F. Pan, B. Cowsill, J.R. Lu, Langmuir 27 (2011) 7654–7662.
[6] S. Chen, L. Liu, J. Zhou, S. Jiang, Langmuir 19 (2003) 2859–2864.
[7] M.E. Wiseman, C. Frank, Langmuir 28 (2012) 1765–1774.
[8] A. Makky, T. Berthelot, C. Feraudet-Tarisse, H. Volland, P. Viel, J. Polesel-Maris, Sens. Actuators B 162 (2012) 269–277.
[9] P. de Thier, J. Bacharouche, J. Duval, S. Skali-Lami, G. Francius, Biochim. Biophys. Acta 1854 (2015) 138–145.
[10] K. Gajos, M. Angelopoulou, P. Petrou, K. Awsiuk, S. Kakabakos, W. Haasnoot, A. Bernasik, J. Rysz, M.M. Marzec, K. Misiakos, I. Raptis, A. Budkowski, Appl. Surf. Sci. 385 (2016) 529–542.
[11] (a) K. Awsiuk, A. Budkowski, P. Petrou, A. Bernasik, M.M. Marzec, S. Kakabakos, J. Rysz, I. Raptis, Colloids Surf. B 103 (2013) 253–260; (b) ibid. 90 (2012) 159–168.; (c) ibid. 11 (2013) 217–224.
[12] V. Lebec, S. Boujday, C. Poleunis, C.M. Pradier, A. Delcorte, J. Phys. Chem. C 118 (2014) 2085–2092.
[13] A.K. Trilling, J. Beekwilder, H. Zuilhof, Analyst 138 (2013) 1619–1627.
[14] N. Tajima, M. Takai, K. Ishihara, Anal. Chem. 83 (2011) 1969–1976.
[15] V. Pagkali, P.S. Petrou, A. Salapatas, E. Makarona, J. Peters, W. Haasnoot, G. Jobst, A. Economou, K. Misiakos, I. Raptis, S.E. Kakabakos, J. Hazard, Mater (2016) http://dx.doi.org/10.1016/j.jhazmat.2016.03.019.
[16] S. Muramoto, J. Brison, D.G. Castner, Anal. Chem. 84 (2012) 365–372.
[17] H.R. Philipp, J. Electrochim. Soc. 120 (1973) 295–300.
[18] J.A. Howarter, J.P. Youngblood, Langmuir 22 (2006) 11142–11147.
[19] J. Kim, J. Cho, P.M. Seidler, N.E. Kurland, V.K. Yadavalli, Langmuir 26 (2010) 2599–2608.
[20] J.H. Wang, J. Am. Chem. Soc. 76 (1954) 4755–4763.
[21] K. Rezwan, L.P. Meier, M. Rezwan, J. Vörös, M. Textor, L.J. Gauckler, Langmuir 29 (2004) 10055–10061.
[22] K.B. Lee, S.J. Park, C.A. Mirkin, J.C. Smith, M. Mrksich, Science 295 (2002) 1702–1705.
[23] J. Buijs, J.W. Lichtenbelt, W. Norde, J. Lyklema, Colloids Surf. B 5 (1995) 11–23.
[24] Universal Protein Resource. http://www.uniprot.org. (Accessed 22 April 2015) ID: P01012 and P02769.
[25] A.P. Cuypers, J.W. Corsel, M.P. Janssen, J.M. Kop, W.T. Hermens, H.C. Hemker, J. Biol. Chem. 258 (1983) 2426–2431.
[26] X.V. Eydne, P. Bertrand, Appl. Surf. Sci 141 (1999) 1.
[27] Y.-P. Kim, M.-Y. Hong, H.-K. Shon, D.-W. Moon, H.-S. Kim, T.-G. Lee, Appl. Surf. Sci. 252 (2006) 6801.
[28] M. Rabe, D. Verdes, S. Seeger, Adv. Colloid Interface Sci. 162 (2011) 87–106.
[29] Z. Adamczyk, Curr. Opin. Colloid Interface Sci. 17 (2012) 173–186.
[30] M.S. Wagner, D.G. Castner, Langmuir 17 (2001) 4649–4660.
[31] E. Kosobrodova, R.T. Jones, A. Kondyurin, W. Chrzanowski, P.J. Pigram, D.R. McKenzie, M.M.M. Bilek, Acta Biomater. 19 (2015) 128–137.
[32] F. Liu, M. Dubey, H. Takahashi, D.G. Castner, D.W. Grainger, Anal. Chem. 82 (2010) 2947–2958.
[33] J. Zhou, H.-K. Tsao, Y.-J. Sheng, S. Jiang, J. Chem. Phys. 121 (2004) 1050.
[34] K. Awsiuk, A. Budkowski, P. Petrou, M.M. Marzec, M. Biernat, T. Jaworska-Gołąb, J. Rysz, Colloids Surf. B 148 (2016) 278.